JOURNAL OF MATERIALS SCIENCE 35 (2000) 5147–5156

An investigation on chain mobility in solid state polymer systems

J. LOOS, M. TIAN, S. RASTOGI, P. J. LEMSTRA
Eindhoven Polymer Laboratories/The Dutch Polymer Institute (DPI), Eindhoven University of Technology, Department of Chemical Engineering, P.O. Box 513, 5600 MB Eindhoven, The Netherlands
E-mail: s.rastogi@tue.nl

In this paper we have investigated chain mobility in polyethylene below its melting temperature. The investigation techniques like atomic force microscopy (AFM), transmission electron microscopy (TEM), time-resolved small/wide angle X-ray scattering (SAXS/WAXS), time-resolved longitudinal acoustic mode (LAM) Raman spectroscopy have been used to follow the chain mobility within individual single crystals and regularly stacked crystals, as a function of temperature and time. Our observations on single crystals are that crystal thickness increases immediately on heating just above the crystallization temperature. In the regularly stacked polyethylene single crystals wherever the overlapping of at least two lamellae arises, thickening occurs during annealing via a mutual chain rearrangement between the adjacent crystals, which leads (ultimately) to a quantum increase, i.e., doubling, of the lamellar thickness. A model has been proposed to explain this quantum increase in the lamellar thickness. The fundamental findings have been extended for some applications.

1. Introduction

In the area of polymer science, important disciplines are polymer physics, concerning the properties of solid polymers, and rheology, concerning the properties of polymer melts. In the past, there has not been a lot of interaction between research groups working in the area of polymer rheology and solid-state properties, respectively. Polymer rheology, in the past two decades of the last century, has been dominated by the concept of chain reptation, viz. chains moving in a virtual tube, and the related, but earlier, concept of a physical entanglement network.

The numerous studies concerning the solid-state properties of polymers can be subdivided into two domains, amorphous vs. semi-crystalline polymers, respectively. In the case of amorphous polymers, the concepts of polymer rheology have been adopted and, for example, a physical entanglement network has been assumed to explain the deformation behaviour of amorphous polymers in the solid state. Well-known studies have been performed by Kramer *et al*. [1] concerning the deformation of amorphous polymers in the solid-state, focusing on the maximum drawability in relation with stretching molecular segments between entanglement loci.

In the case of semi-crystalline polymers, the phenomenon of chain folding attracted the attention of many scientists, since its discovery by Keller and Fischer in the mid-fifties of the last century. The way chains are folding back and forth in a platelet-like (lamellar) single crystal was studied in detail for the case of linear polyethylenes, notably for crystallisation from very dilute solutions and at low supercoolings. Crystallisation from dilute solutions, viz. of isolated polymer chains, is now rather well documented, albeit vigorous discussions are still prevalent concerning the details of chain-folding, adjacent vs. switchboard models. Crystallisation from the melt is much more difficult to understand, in view of highly entangled chains in the molten state and restricted motions (reptation). Theories have been proposed concerning reeling-in of polymer chains onto the crystal surface, viz. disentangling of chains from their 'tubes'.

The reverse process of crystallisation is melting, the transition from the solid-state to the melt, and, recently, intriguing observations have been made by us and other groups. For the sake of later discussions, we recapitulate the salient observations:

1. Solution-grown and well-developed single crystals of polyethylene, in our studies ultra-high-molecular-weight linear polyethylenes (UHMW-PE), sedimented into single crystal mats are very ductile and can be drawn in the solid state to very high draw ratios (in a temperature range close to but clearly below the melting temperature). These favourable drawing characteristics are related to a reduced entanglement-density in these single crystal mats, compared with crystallisation from the melt;

2. The favourable drawing characteristics are lost instantaneously when the single crystal mats are heated

above the melting temperature and re-crystallised from the molten state;

3. Rheological measurements as a function of time, after melting these single crystal mats, did not show any memory effect as anticipated from melting disentangled high molar mass polyethylenes;

4. Parallel measurements concerning the radius of gyration upon melting show a jump, from a compact chain conformation in the crystalline state to a random coil upon melting, referred to as 'chain-explosion' upon melting;

5. Annealing of single crystal mats below the melting temperature show a quantum jump increase in lamellar thickness (doubling) *without* loss in drawability;

6. Nascent UHMW-PE reactor samples, possessing also folded-chain crystals as a consequence of crystallisation simultaneously with polymerisation, show an unusually high melting temperature, viz. 141–142°C, which is equal to the equilibrium melting temperature of polyethylene!

The observations and experimental findings, listed above, could provide insight in molecular mobility, not only for the solid-state but equally well for the polymer melt as will be discussed below, in combination with new experimental findings. To have a further insight at the molecular level for the above quoted findings, in this paper we will follow the chain mobility within a crystal as a function of temperature and time in single crystals and regularly stacked lamellae using investigation techniques like atomic force microscopy (AFM), transmission electron microscopy (TEM), time-resolved small/wide angle X-ray scattering (SAXS/WAXS), time-resolved longitudinal Acoustic mode (LAM) Raman spectroscopy. The fundamental findings will be extended for some applications, like overcoming the problem of chain reptation time in welding process of UHMW-PE and an explanation for the high melting temperature normally observed in nascent UHMW-PE powders.

2. Experimental

2.1. Single crystal preparation and handling

The material used in the first section of this study was kindly provided by Phillips Petroleum Comp., USA (linear PE with $M_w \sim 100$ kg/mol, $M_w/M_n \sim 1.04$). Individual single crystals were prepared by isothermal crystallization of dilute solutions of PE in xylene ($\sim$0.01 wt%) at various temperatures. To ensure fairly uniform crystal size and shape, the technique of self-nucleation was followed [2]. Single crystals were annealed after deposition on cleaved mica and subsequently investigated by AFM.

In-situ AFM investigations during annealing of the samples were performed using a PicoSPM^{TM}, (Molecular Imaging Corp, USA), which is specially designed for scanning force microscopy measurements in controlled environment and equipped with a hot-stage. *Ex-situ* AFM investigations of single crystal samples were performed using a Dimension 3100, Digital Instruments, Inc., (Santa Barbara, California). The mica substrates were scratched with a scalpel to ease the repeated search of the same sample area by means of the optical microscope, which is integrated in the AFM. Further position refinement of the analysed area was performed by AFM imaging using the coordinates of some characteristic landmarks in the surface. Between two successive AFM observations, the samples were placed onto a Linkam THMS600 hot-stage to perform the annealing treatment for defined temperatures and times. The AFMs were calibrated using height standards produced by Silicon-MDT Ltd., Russia.

2.2. Single crystal mats and handling

Solution-crystallized single crystal mats were obtained by dissolving UHMW-PE ($M_w \sim 3 \times 10^3$ kg mol^{-1}, kindly provided by Hoechst AG, Germany) at 135°C in xylene. To avoid air bubbles in the mats, the solvent was degassed and flushed with nitrogen gas to prevent oxidation. The polymer concentration was 1% by weight. After dissolution, the hot solution was quickly transferred to an aluminium tray and left to cool slowly under quiescent conditions. Upon cooling, a gel is formed and the wet gel is stapled onto a cardboard to prevent lateral shrinkage. The gel is left to dry. This process took about 1 week, and we anticipate no xylene is left in the dried gel. The dry mats thus formed were subjected to the experimental investigations. The described method to prepare single crystal mats is discussed in detail elsewhere [3].

Small and wide angle X-ray scattering (SAXS/WAXS) studies on these samples were performed at the station 8.2 of the synchrotron radiation facility available in Daresbury, U.K. [4]. A Linkam THMS 600 hot-stage mounted on the optical bench with a sample holder (capillary/film) was used to perform heating, cooling or annealing experiments. The SAXS and WAXS detectors were calibrated using the usual standards. The experimental data were normalized for the transmitted intensity, corrected for detector response and the background scattering.

LAM Raman spectra from the UHMW-PE mats were obtained *in-situ* using a Dilor, France, triple monochromator spectrometer. An Argon laser was used. The frequency shift of a peak with respect to the excitation line, denoted by $\Delta\nu$, expressed in cm^{-1} throughout the text, can be converted into values for the chain length within the crystalline region using the relationship derived by Schaufele and Schimanouchi [5] for *n*-alkanes. For polyethylene, a Raman chain length, L_R, can directly be calculated from the first order frequency shift by using the expression $L_R = 3169/\Delta\nu$. The morphology of the not annealed and annealed solution-crystallized films was examined using a Jeol JEM 2000FX transmission electron microscope.

3. Results

3.1. AFM investigations of individual PE single crystals

The thickness of polyethylene single crystals prepared from dilute solution depends on the crystallization

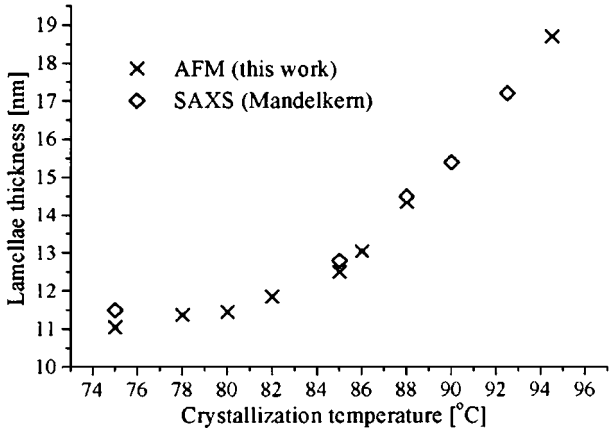

Figure 1 Plot of the single crystal thickness versus crystallization temperature. SAXS data are from Ref. [6].

temperature: with increasing temperature the lamellae become thicker. Lamellar thicknessess measured for different crystallization temperatures are summarized in Fig. 1. Inserted are additional data from SAXS experiments performed by Mandelkern *et al*. [6]. AFM height data of single crystals represent always the core crystal thickness (L_C) together with the amorphous layers coated on both sides. Our thickness data scatter in the order of ± 0.4 nm and are calculated, as indicated, on the basis of measurements of several crystals grown from different solution batches. Taking the error range into account, our data match with the well established and often confirmed SAXS data. Thus, thickness measurement of PE single crystals using AFM must be considered as accurate.

Typical AFM images (in height contrast) corresponding to the evolution of isolated as well as stacked individual single crystals before and after annealing are presented in Fig. 2. The images are recorded *ex-situ*, the sample is annealed for 30 min at each temperature in a hot-stage, subsequently cooled to room temperature, and repositioned in the AFM. *In-situ* investigations produce identical morphological changes and thickness data; however, the quality of those images is somewhat lower, and they are not shown here. The single crystals are originally grown at 85°C and have a thickness of ∼12.3 nm and ∼25 nm for regions where two crystals are overlapped, respectively. The morphology of single crystals annealed slightly above the original crystallization temperature seems to be unchanged except for a few surface features, which will be discussed in detail in a separate study [7].

Distinct changes appear at different annealing temperatures in the range between the original crystallization temperature and ∼120°C (Fig. 2b and c). The annealed samples show appearance of cavities widely spread over the surface of a crystal, giving rise to Swiss Cheese like morphology. However, the shape of lamellae stays the same before and after annealing. It is to be noted that the regions where two lamellae overlap no formation of cavities is observed. The described regions are marked as A for the individual lamellae and B for the overlapped lamellae as shown in Fig. 2.

Beside the observed morphological changes as described above the lamellae thickness of individual

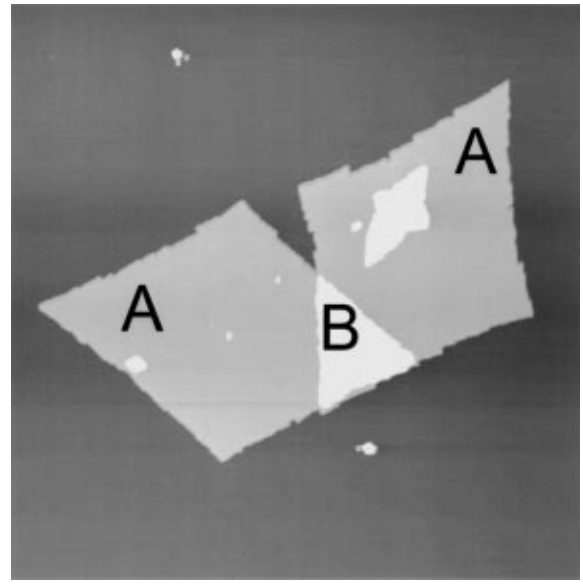

(a)

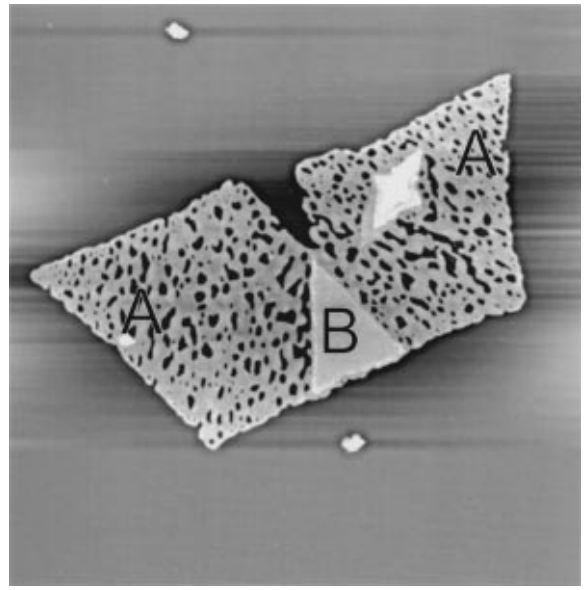

(b)

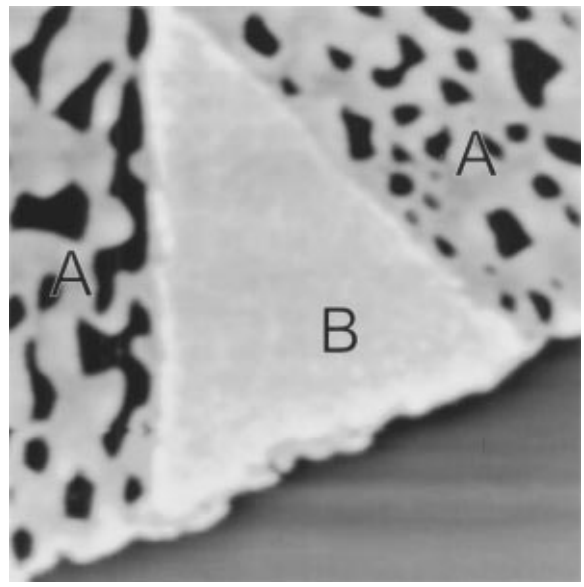

(c)

Figure 2 Height mode images of partially overlapping individual lamellae recorded a) as-crystallised at 85°C and b) after annealing at 110°C; c) higher magnification of the overlapping region of a). The regions of individual and overlapped lamellae are marked as A and B, respectively.

lamellae increases continuously with increasing annealing temperature, whereas the overlapped regions (B in Fig. 2) keep their original thickness constant, independent of the annealing temperature and time. We have measured the thickness evolution on annealing of single crystals originally grown at temperatures between 78°C and 95°C. The average thickness data upon annealing show always the same trend. To summarise, the thickness of the individual lamellae increases just above the crystallization temperature, whereas the thickness of stacked lamellae remains unchanged, independent of the annealing temperature.

3.2. Investigations of films possessing well-stacked UHMW-PE single crystals mats

The observations reported on single crystals have been extended to regularly stacked lamellae. Well-defined regularly stacked lamellae are observed in solution-crystallised films of UHMW-PE [3, 8]. Fig. 3 shows the time resolved SAXS patterns while heating the solution-crystallised film at a rate of 10°C/min. At low temperatures, the SAXS patterns show three peaks with decreasing intensity along the scattering wave number q, satisfying the Bragg's condition for the first ($q = 0.52$ nm^{-1}), second ($q = 1.04$ nm^{-1}), and third ($q = 1.56$ nm^{-1}) order of an average lamellar thickness of ~12 nm. The higher orders and sharp peaks in SAXS patterns suggest regular stacking of lamellae with narrow thickness distribution. This is confirmed by TEM (Fig. 4a). On heating above the threshold temperature of 110°C, initially a broad weak peak at q = 0.262 nm^{-1} ($d \sim 24$ nm) appears. This peak becomes sharper and more intense, with diminishing intensities of the second and third orders and a simultaneous decrease in intensity of the first order for the original 12 nm crystals. The increase in lamellar thickness corresponds to a major rearrangement of chains, as confirmed by TEM in the annealed sample (Fig. 4b). It is evident that the thickness of the majority of the lamellar crystals increases to twice the initial value.

Fig. 5 shows a schematic representation of the increase in lamellar thickness with temperature, plotted from the SAXS observations. The changes observed in lamellae thickness with temperature may be divided into three different regions: AB, BC and CD. Within region AB, the lamellar thickness is constant, whereas in region BC, shown by the dotted line, two different populations in terms of lamellar thicknesses (i.e. 12 nm and 24 nm) exist together. Our observations are that above a temperature of 110°C the lamellae start to thicken to double the initial value. After doubling a logarithmic increase in lamellar thickness is observed during annealing or heating, defined as Region CD in Fig. 5.

The region BC in Fig. 5 is of significance to evaluate the mechanism involved in lamellar thickening. Therefore, it is of interest to investigate the influence of annealing within this region. The SAXS data of a heating scan from 75°C to 115°C at the rate of 5°C/min are presented in Fig. 6a. Above 110°C, a few lamellae in the bulk thicken to double the initial value, while the remaining crystals do not change in terms of thickness. Thus, in the bulk of the sample two distinct populations of lamellar thicknesses exist together. When the sample is left to anneal at 115°C, the peak intensity for the 12 nm crystals decreases, while a simultaneous increase in the peak intensity for the 24 nm crystals occurs (Fig. 6b). The rate of increase depends on the annealing temperature. When the sample is heated further beyond the annealing temperature at a rate of 1°C/min, an

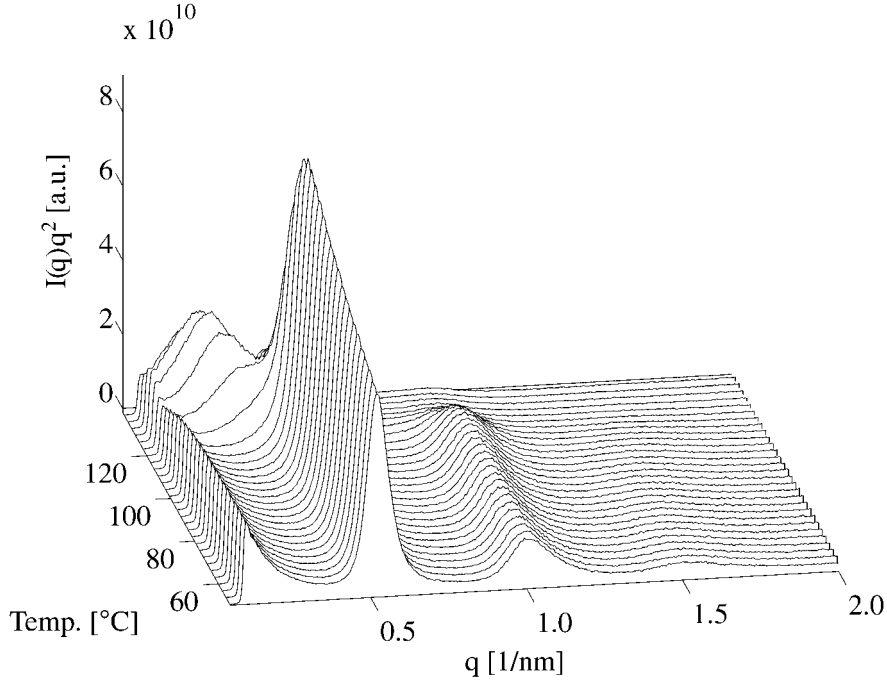

Figure 3 SAXS patterns of a solution-crystallised UHMW-PE film during a heating scan from 25°C to 140°C at 10°C/min. Where $q = 2\pi/d$; d is the average lamellar thickness.

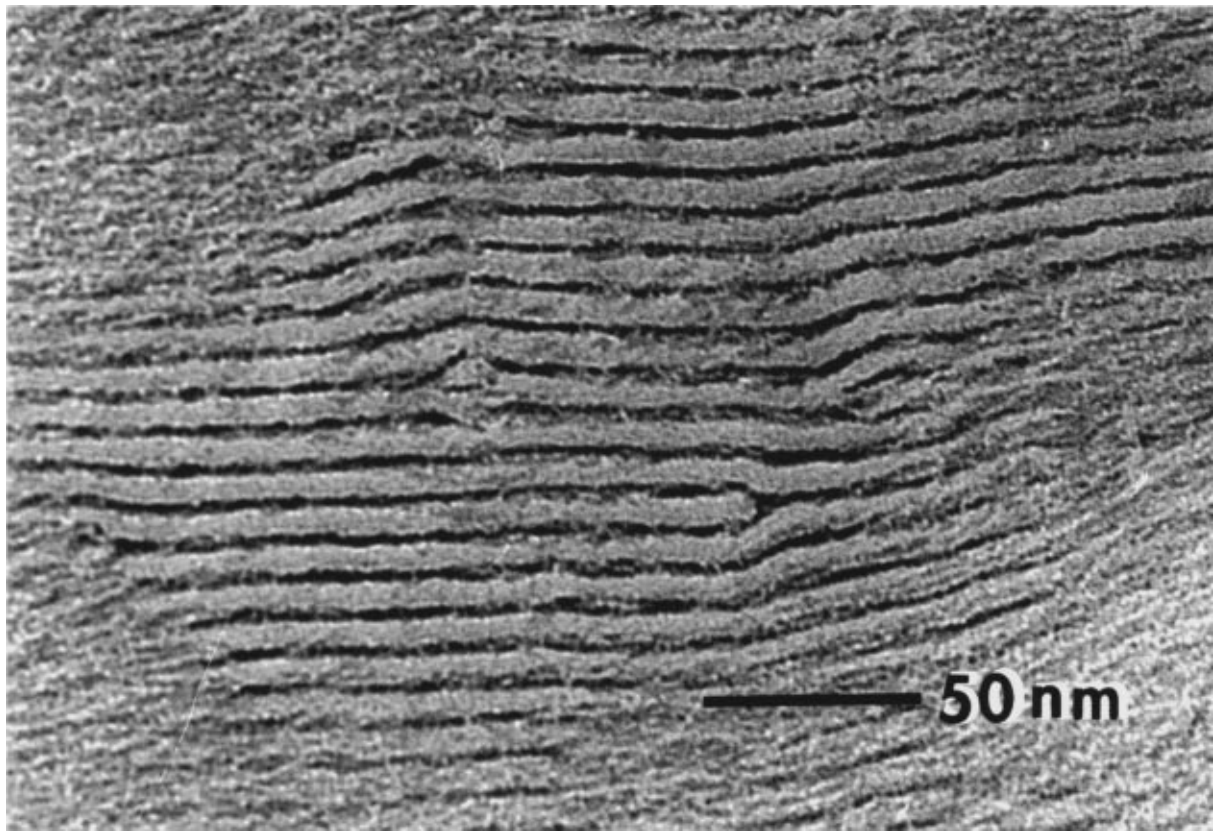

(a)

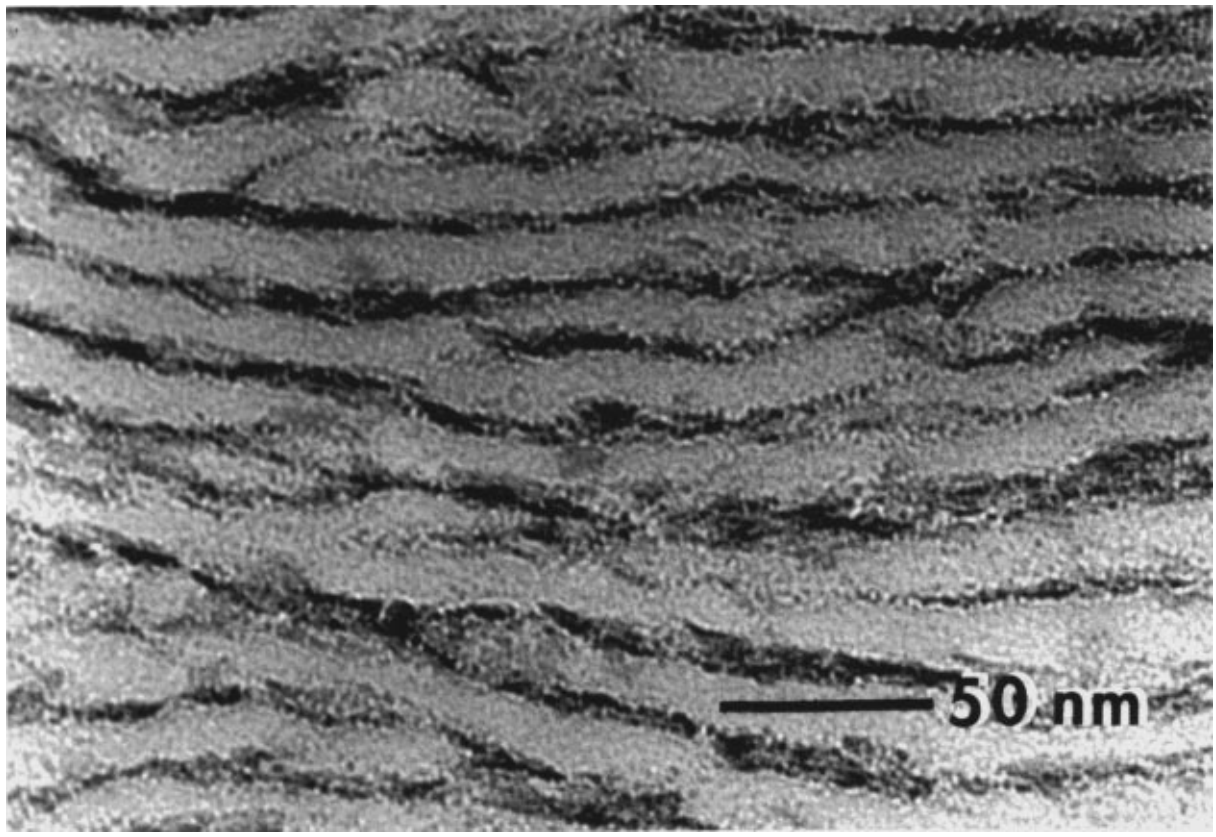

(b)

Figure 4 (a) TEM of solution crystallised UHMW-PE film. (b) TEM of the film annealed at 125°C for 15 minutes. Bands are lamellae as viewed edge-on.

increase in the peak intensity from 24 nm lamellae occurs, whereas the peak of the 12 nm lamellae disappears totally (Fig. 6c). The lamellae melt at ∼135°C without any substantial thickening beyond 24 nm. These results clearly demonstrate that within region BC of Fig. 5 only two distinct populations of the crystals exist, favouring the quantised thickening in the regularly stacked lamellae.

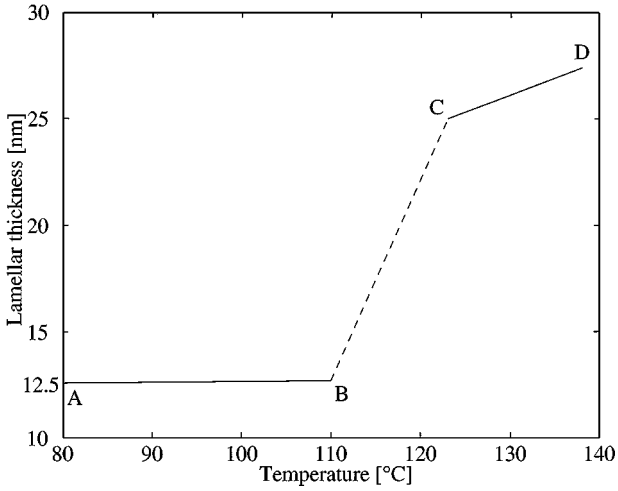

Figure 5 A schematic representation of the increase in the lamellar thickness as function of temperature.

From the *in-situ* SAXS patterns alone, it is clear that the lamellar thickness increases on heating to twice the initial value (doubling), but no conclusion on the mechanism involved could be made. It may occur either via interchain diffusion between the neighbouring crystals [9], via an increase in the amount of amorphous material in between the crystalline core [10] (i.e., premelting of selective small lamellae within the lamellar stacks or surface melting of the crystals) or via a melting and recrystallisation process [6]. All these mechanisms would lead to development of the SAXS pattern as observed. To investigate the mechanism involved during chain rearrangement in the crystalline core, we have performed *in-situ* LAM Raman experiments at elevated temperatures. As stated earlier, by this technique one may follow the chain motion within the crystalline core.

Before application of this technique to our experimentation, it is important to investigate the influence of temperature on LAM Raman in general. This has been done and details have been published elsewhere [3], a summary of the results is given below. So far, there has not been much effort to use LAM Raman as a tool to reveal chain arrangement in detail at temperatures higher than room temperature.

Since the SAXS pattern does not show any substantial shift during annealing of the solution-crystallised film in the regions AB and CD (as described above), we made use of such an annealed film to investigate the shift in LAM Raman due to temperature. Therefore, the observed LAM Raman peaks at $\sim$26.4 cm^{-1} and $\sim$13.2 cm^{-1} can be assigned to lamellar thicknesses of 12 nm and 24 nm (Fig. 7), respectively. It may be noticed that on heating below the melting temperature neither the peak position of the 13.2 cm^{-1} band shifts nor broadens. Close to the melting temperature, only a drop in the intensity with an asymmetric broadening of the LAM Raman peak towards higher frequencies occurs.

A set of Raman spectra collected at different temperatures is shown in Fig. 8a. The original sharp peak at 26.7 cm^{-1} broadens and moves to lower frequencies above a threshold temperature of 110°C. The peak shifts gradually from 26.7 cm^{-1} to 13.2 cm^{-1} with increasing temperature. The maximum shift to 13.2 cm^{-1} is observed at approx. 130°C where the peak strengthens in intensity. On cooling, from 130°C to room temperature, the band at 13.2 cm^{-1} strengthens in intensity and becomes more distinct, as shown in Fig. 8b in comparison with the unannealed film. From the presented set of experiments it is clear that the crystalline core increases in thickness above the threshold temperature of

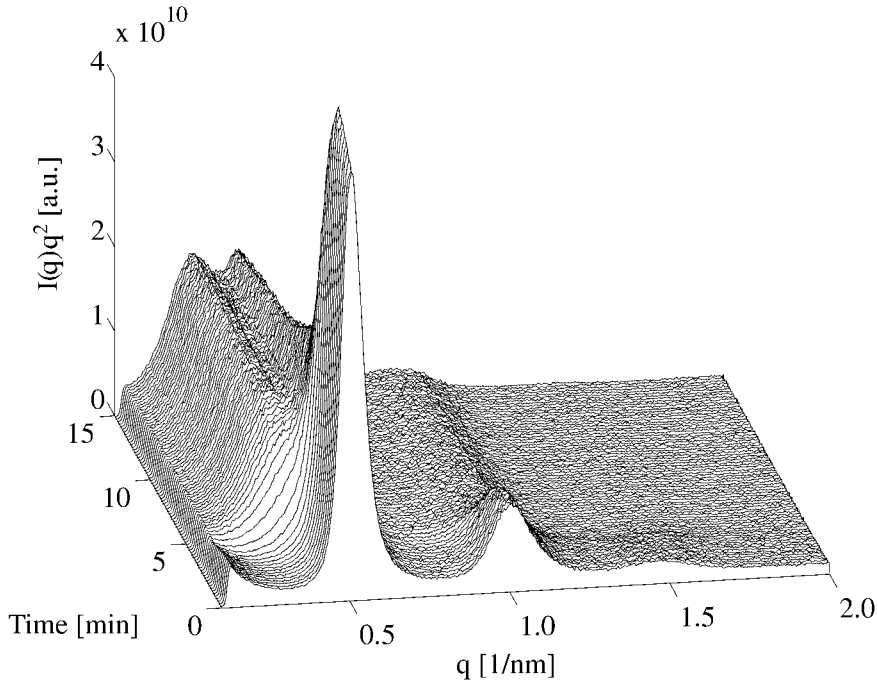

(a)

Figure 6 Time resolved SAXS patterns obtained during: (a) a heating scan from 75 to 115°C at 5°C/min (0–8 minutes) and left to anneal (8–15 minutes), (b) annealing for 15 minutes at 115°C, and (c) a heating scan from 115 to 140°C at 1°C/min. Where $q = 2\pi/d$; d is the average lamellar thickness. (*Continued*)

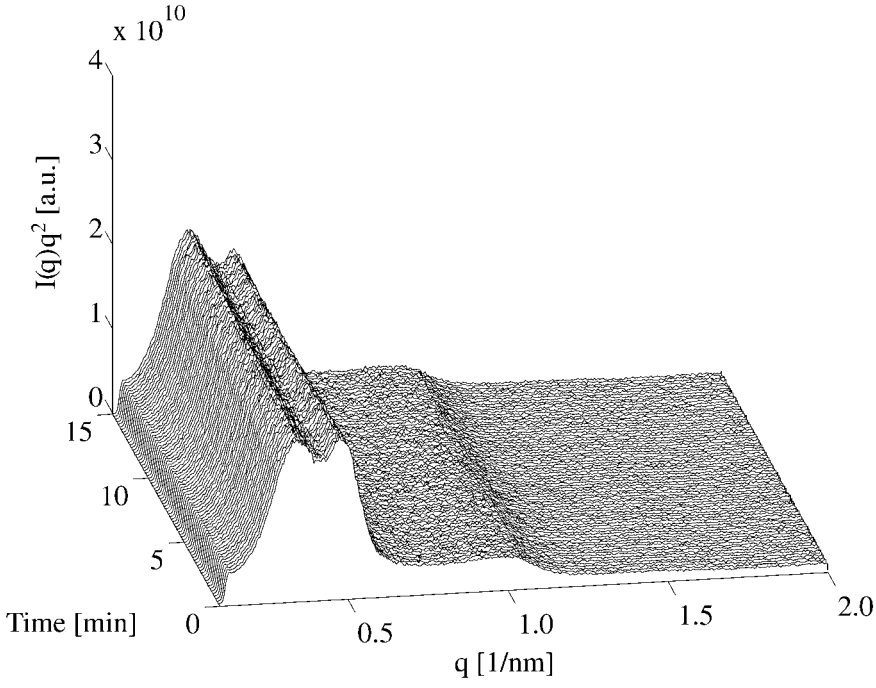

(b)

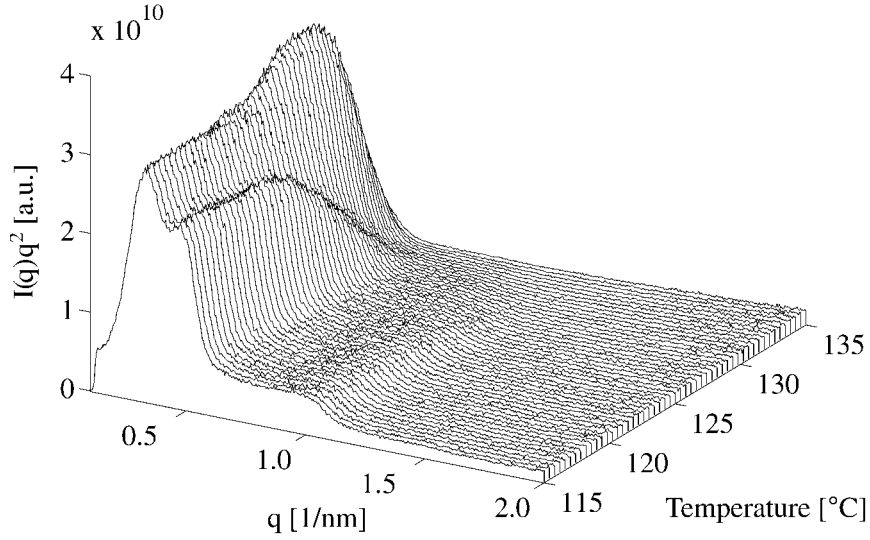

(c)

Figure 6 (*Continued*).

110°C to twice the initial value. The continuous shift in the LAM Raman peak to lower frequencies cannot be associated with the melting of alternate lamellae or the crystalline core.

4. Discussion

High chain mobility in the solid state below the melting point is well established for polyethylene when a sample is annealed within the hexagonal phase, a phase accessible at high temperatures and pressures [11–13]. Because of the enhanced chain mobility extended chain crystals can be formed. Overall crystallinity of the sample increases to nearly 100%, changing the mechanical property of the sample from tough to brittle.

In our studies reported here the morphological changes on annealing the sample, below the melting temperature, are caused because of lamellae thickening in the individual as well as regularly stacked crystals within the orthorhombic phase. The origin of such a change is a consequence of high chain mobility of the molecules along the *c*-axis. The thermodynamic driving force, for the thickening, is the reduction of the Gibbs free energy from folded to extended chain crystals. The molecular stems move along the crystallographic *c*-axis, with a cooperative pulling and pushing of neighbouring stems via the chain loops, whereas mobility in the lateral direction does not occur.

Beside the high chain mobility in the crystalline phase a quantum increase in lamellar thickness has also been observed in sharp fractionated *n*-alkanes [14], low molecular weight poly(ethylene oxide) [15, 16], block copolymers (poly(ethylene oxide)/polystyrene) [17] and single crystals of nylon 6,6 [9]. The quantum

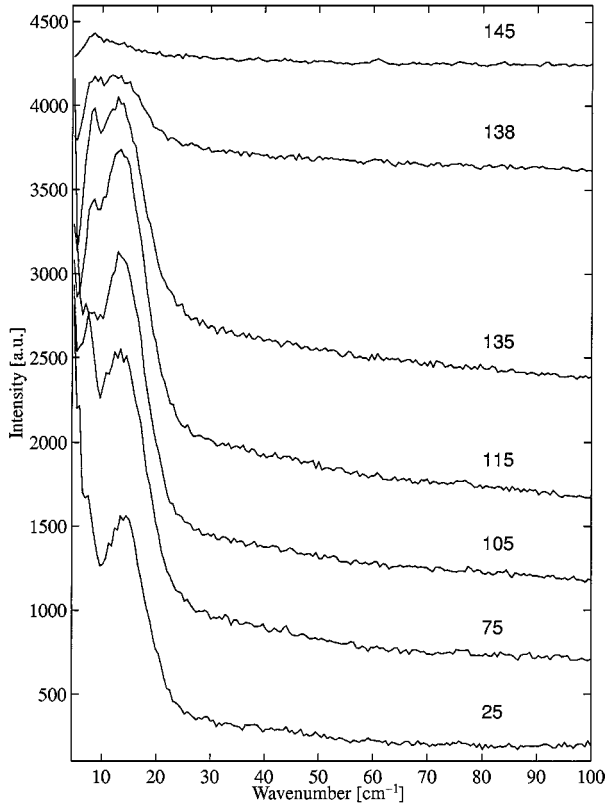

Figure 7 2-D plot of the LAM Raman spectra obtained during a heating scan from 25 to 145°C at 5°C/min of an annealed solution-crystallised film. The temperatures are plotted in the figure.

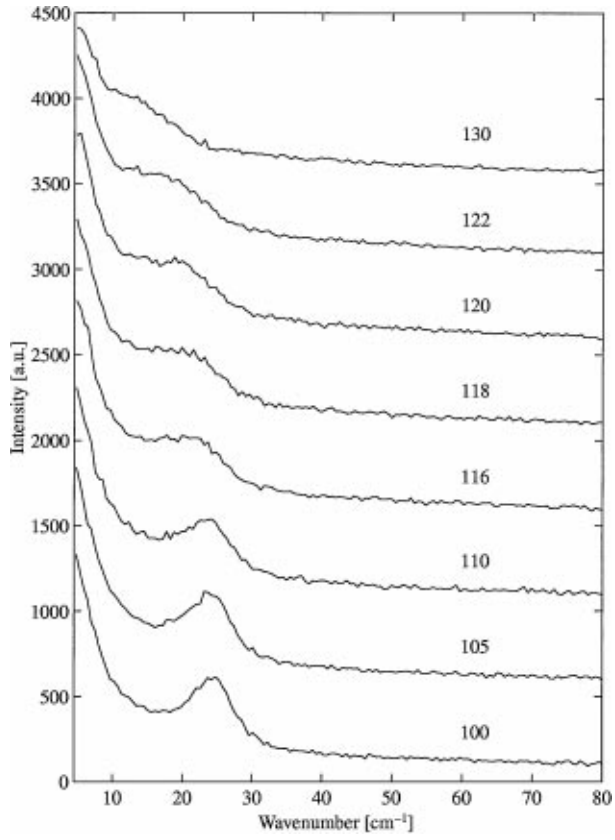

(a)

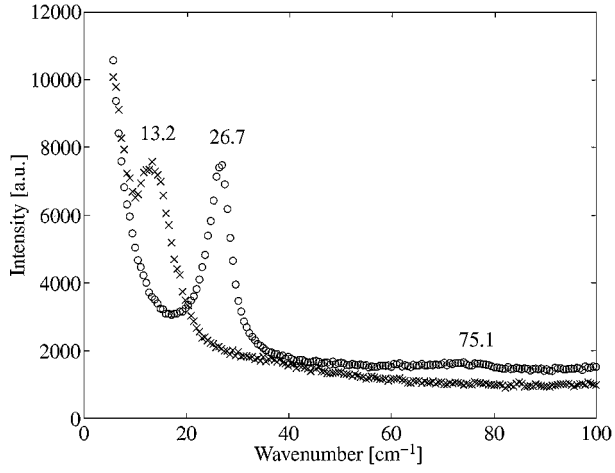

(b)

Figure 8 (a) 2-D plot of representative temperatures during this heating scan (b) Comparison of the LAM measured at room temperature between an unannealed and annealed film. (o represents the unannealed film, x represents the annealed film).

increase in the thickening during the very initial stages of crystallisation in sharp fractionated polyethylene from the melt [18] has also been reported.

One of the common morphological features, wherever the quantum increase in lamellar thickness is observed during annealing or heating below the melting temperature, is that the bulk of the material contains regularly stacked lamellae. A comparison between *n*-alkanes, PE and UHMW-PE shows that the quantum increase in thickening process is independent of the molecular weight. This suggests that the mutual chain rearrangement between the adjacent crystals is a cooperative phenomenon where certain localised chain segments are involved rather than the whole chain. Conformations thus generated in the thickening region tend to move rapidly in and out of the crystal lattice and transport dislocations out to minimise the energy.

A doubling scheme for the chain rearrangement between the adjacent crystals leading to doubling of the fold length has been also proposed by Dreyfuss and Keller for nylon 6,6 [9] and thereafter suggested by Barham and Keller [18] in the case of isothermal crystallisation of polyethylene, i.e., primary thickening. With the help of neutron scattering, Sadler investigated the dimensions of individual molecules and changes in relative positions of different molecules during the annealing of solution-grown single crystals of polyethylene [19]. On following the chain trajectory of the deuterated molecule, it was found that on annealing at 123°C or lower the dimensions normal to the crystal lamellae increase in line with the lamellar thickness. During the thickening process the dimensions in the lateral direction of the crystallites were found to remain constant.

Taking the literature and our own results into account, the following model is proposed for the quantum increase in the lamellar thickness. The mechanism of the doubling process will be explained in view of the experimental details. Fig. 9a shows a schematic drawing of regularly stacked lamellae. Once the film is heated above the temperature region of the α-relaxation, which dependents on the original crystals thicknesses, the thermodynamic driving force for lamellar thickening, minimisation of Gibbs free energy, will cause the chains to slide within the lamellae to come to their final state.

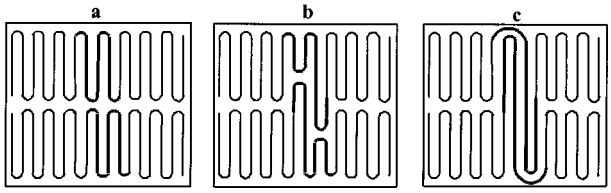

Figure 9 A schematic model to explain the doubling phenomenon in the regularly stacked adjacent lamellae. The bold line represents the test chain.

The sliding chain within one lamella may push the chain in the adjacent lamella cooperatively, as shown schematically by the bold line, representing the test chain in question (Fig. 9b). For the sake of simplicity we have refrained ourselves to the selected region of the crystals. Defects and conformations, associated with the (fold) surface, which are dynamically incorporated into the crystal lattice during chain sliding, will be removed again once the crystal thickness has increased because of energetic reasons. From the model (Fig. 9c), it is evident that once the doubling process is brought to an end, chains get mutually entangled at the surface and further thickening via joint chain rearrangement between the adjacent crystals cannot occur.

An additional increase in lamellar thickness, which is logarithmic with time, should occur via dynamic melting and a recrystallisation process. In this respect our model is rather different than the one proposed by Keller and co-workers [9, 18] in which thickening can occur in quantum jumps not only doubling but also up to quadrupling.

5. Conclusions

From the above set of experiments the following conclusions could be drawn:

1. Our observations on single crystals suggest that on heating just above the crystallisation temperature crystal thickness increases immediately.
2. In the regularly stacked polyethylene single crystals, thickening occurs during annealing via a mutual chain rearrangement between the adjacent crystals, which leads (ultimately) to a quantum increase, i.e., doubling, of the lamellar thickness. Our proposed model can explain this quantum increase in the lamellar thickness.
3. After the doubling process is completed, further thickening via mutual chain rearrangement is hindered due to the fact that chains at the surface get entangled (switch board) and, moreover, the regular stacking of lamellar crystals is lost. Further thickening of the doubled lamellar crystals involves a process of surface melting or melting and re-crystallisation.

As the lamellar thickening is an activated process the rate of increase, ultimately leading to the quantum increase, will depend on the annealing temperature, i.e., at the higher temperatures, the doubling process will be faster.

5.1. Applications to welding

With the help of the model proposed in Fig. 9, the adjacent re-entry leading to welding of two crystals within region B of Fig. 2 can be also explained. Above we also stated that independent of the molecular weight lamellae thickness increases by double the initial value. Now the question arises, can we make use of the proposed doubling mechanism for the welding of two films of UHMW-PE, thus overcoming the problem of reptation time ($\tau \sim M^3$) in welding process. In the quest to answer the question we have performed a series of experiments and a summary of the results is stated below.

Making use of the concepts outlined above our recent findings [20] suggest that the lamellar doubling process could be used to introduce a well-defined amount of co-crystallisation across the interface, by annealing two stacked completely wetted solution-crystallised films. The experimental observations are that doubling of the lamellae across the interface enhances the peel energy of the two films of UHMW-PE to such a level, that the films could not be separated anymore. By contrast, reference samples, in which co-crystallisation across the interface was prohibited by pre-annealing one side of the film, could still be separated easily. In this example, the enhanced chain mobility was used to overcome the basic fundamental problem arising in welding of the two films of UHMW-PE.

5.2. Crystal size dependence in lamellae thickening

Above we have also quoted that when crystals are isolated thickening occurs immediately above the crystallisation temperature as shown in Fig. 2. The experiments performed in our laboratory also suggest that the initial morphology of UHMW-PE, can be controlled by the polymerisation conditions like temperature and the catalyst used for the purpose. In simple terms, if the polymerisation temperature is lower than the crystallisation temperature a growing chain on the catalyst surface will crystallise immediately. The ultimate polymerisation conditions can result into isolated crystals, eventually leading to monomolecular crystals where a single chain forms a single crystal. Thus obtained fully disentangled chains when subjected to heat treatment will lead to a thickening process and ultimately resulting a high melting temperature close to the equilibrium melting point. As explained above for the single crystals the thermodynamic driving force for the chain extension is the minimisation of the Gibbs free energy [21, 22].

Acknowledgement

The authors are grateful for financial support from The Dutch Polymer Institute (DPI). Helpful discussions with Bernard Lotz, Jürgen Petermann and Günther Höhne are appreciated. The authors also wish to thank Joachim Koenen (WiTec GmbH, Germany) and Ute Schmidt (Molecular Imaging Corp., USA), who made the PicoSPM available. The authors wish to thank for the availability of the facilities at Station 8.2 of the

Synchrotron Radiation Source (SRS), Daresbury, UK, and at Beamline ID-11/BL-2 of the European Synchrotron Radiation Facility (ESRF), Grenoble, France. Further, the authors are thankful for the experimental facilities available at Dilor, Lille, France for the Raman measurements.

References

1. A. M. DONALD and E. J. KRAMER, *J. Polym. Sci., Polym. Phys. Edn*. **20** (1982) 899.
2. D. J. BLUNDELL, A. KELLER and A. J. KOVACS, *J. Polym. Sci*. **B4** (1966) 481.
3. S. RASTOGI, A. B. SPOELSTRA, J. G. P. GOOSSENS and P. J. LEMSTRA, *Macromolecules* **30** (1997) 7880.
4. W. BRAS, G. E. DERBYSHIRE, A. J. RYAN, G. R. MANT, A. FELTON, R. A. LEWIS, C. J. HALL and G. N. GREAVES, *Nucl. Instr. Meth. Phys. Rev. A* **A326** (1993) 587.
5. R. F. SCHAUFELE and T. SCHIMANOUCHI, *J. Chem. Phys*. **47** (1967) 3605.
6. L. MANDELKERN, R. K SHARMA and J. F. JACKSON, *Macromolecules* **2** (1969) 644.
7. M. TIAN and J. LOOS, *ibid*., submitted.
8. Q. R. ZHU, K. L. HONG, L. Q. JI, R. R. QI, G. E. ZHOU, M. S. SONG and Y. W. WONG, *J. Polym. Sci. B, Polym. Phys*. **33** (1995) 739.
9. P. DREYFUSS and A. KELLER, *J. Macromol. Sci.-Phys*. **B4**(4) (1970) 811.
10. E. W. FISCHER, *Pure Applied Chem*. **31** (1972) 113.
11. B. WUNDERLICH and J. GREBOWICZ, *Adv. Polym. Sci*. **60** (1984) 1.
12. B. C. BASSETT, *Polymer* **17** (1976) 460.
13. S. RASTOGI, L. KURELEC and P. J. LEMSTRA, *Macromolecules* **31** (1998) 5022.
14. G. UNGAR, J. STEJNY, A. KELLER, I. BIDD and I. C. WHITING, *Science* **229** (1985) 386.
15. A. J. KOVACS and C. STRAUPE, *Faraday Disc. Chem. Soc*. **68** (1979) 225.
16. S. Z. D. CHENG and J. CHEN, *J. Polym. Sci. B Polym. Phys*. **29** (1991) 311.
17. A. J. RYAN, manuscript in preparation.
18. P. J. BARHAM and A. KELLER, *J. Polym. Sci. B Polym. Phys*. **27** (1989) 1029.
19. D. M. SADLER, *Polymer Comm*. **26** (1985) 204.
20. Y.-Q. XUE, T. A. TERVOORT, S. RASTOGI and P. J. LEMSTRA, *Macromolecules*, submitted.
21. Y. M. T. ENGELEN and P. J. LEMSTRA, *Polym. Comm* **32** (1991) 343.
22. S. OTTANI, E. FERRACINI, A. FERRERO, V. MALTA and R. S. PORTER, *Macromolecules* **28** (1995) 2411.

Received 10 February
and accepted 22 February 2000